Baseline-Free Defect Detection in Curved Surfaces Using a Neural Surrogate Wavefield Model

GUAN-WEI LEE, JUNGHOON SOHN,
SHIVASHANKAR PERUVAZHUTHI
and SALVATORE SALAMONE

ABSTRACT

Accurate defect localization in structural health monitoring (SHM) can be performed by using high-resolution wavefield data, which can be challenging to obtain due to hardware limitations and time constraints. In this work, we propose a data-driven surrogate model that reconstructs high-resolution wavefields from sparse measurements, enabling efficient and precise defect localization. Our approach leverages a coordinate-based neural network to interpolate waveforms continuously, allowing for theoretically infinite resolution wavefield predictions.

The proposed framework reduces data acquisition demands while preserving the fidelity of wavefield information, making it an efficient tool for SHM. Modeling results using numerical simulation data demonstrate that our approach reconstructs wavefield data and can be used to identify scattering sources associated with defects.

INTRODUCTION

This work is motivated by the need to monitor dry cask storage systems (DCS), which are large stainless-steel cylinders used to store spent nuclear fuel rods. These casks are housed within concrete enclosures and emit high levels of radiation, making direct non-destructive evaluation (NDE) challenging. Robotic-assisted sensor deployment is currently being explored for such environments, where only sparse sensor data may be feasible. In this context, reliable defect localization using limited measurements is highly valuable.

Previous work [1] has demonstrated defect imaging on a full-scale DCS using a baseline subtraction approach, where wavefield data from damaged and undamaged states are compared to identify anomalies. However, this method can be affected by variations in ambient conditions. Differences between the baseline and in-service environments can introduce localization errors, and propagation compensation techniques are only effective if ambient conditions are measured. To overcome these limitations, we propose a baseline-free approach that reconstructs the entire wavefield from sparse measurements. Defects are then identified based on localized scattering patterns in the reconstructed field.

Our method is inspired by sparse-recovery techniques that use phasor solutions as basis functions to fit Lamb wave data [2]. We extend this idea beyond dispersion curve

estimation to learn full wavefield behavior and arrival patterns using a machine learning framework. Specifically, the model captures incident waves, scattered waves, and helical arrivals that travel along the cylindrical surface [1], by fitting sparse sensor readings to a set of complex analytical Lamb wave solutions.

To evaluate the approach, we use a numerical simulation of A0 mode Lamb wave propagation in a pipe with an introduced crack. Incident wave removal [3] is performed on the predicted wavefields to assess the model's ability to reveal scattering energy and localize defects.

The remainder of this paper is organized as follows: the Methodology section describes the basis function, model architecture, and Incident wave removal analysis. The Simulation section details the generation of the dataset. The Results section presents model performance and defect localization outcomes. Finally, the Conclusion discusses limitations, potential improvements, and directions for future work.

METHODOLOGY

The basis function used in this work is a complex analytical solution parameterized to fit observed data. It models the out-of-plane displacement u as

$$u(r,\omega) = a\sum_{i} b * e^{-j((k(\omega_i)r+\varphi)-\omega_i t)} \quad (1)$$

with distance r from the excitation source, angular frequency ω, frequency dependent wavenumber $k(\omega_i)$ and time t. The basis function includes three parameters: (a, b, φ). Specifically, a controls the amplitude scaling, b acts as a windowing parameter on each frequency component that adjusts the width of the wave packet, and φ sets the phase offset. These parameters allow the analytical solution to flexibly represent the shape and timing of Lamb wave packets observed in the data.

The model is designed to predict waveforms at arbitrary spatial coordinates (x, y) using Equation (1), making the model's input a spatial coordinate (x, y) and it outputs the set of parameters (a, b, r, φ). To maintain simplicity, the architecture consists solely of fully connected neural networks. The input coordinates are first projected into a 256-dimensional feature space through three linear layers. Each output parameter is predicted through a separate linear layer with an appropriate activation function to constrain its value within a physically meaningful range. The model architecture is illustrated in Figure 1.

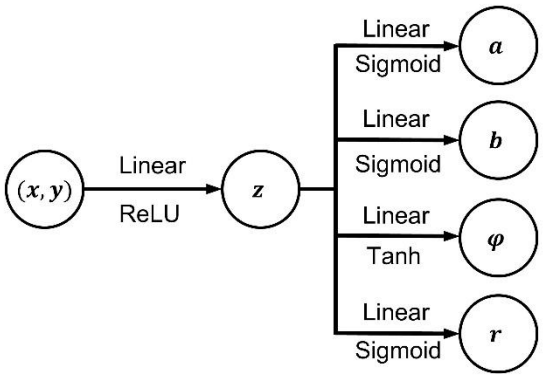

Figure 1. Model Architecture

The ω, t and $k(\omega)$ are predefined with $k(\omega)$ using theoretical values. Careful selection of frequency and time step sizes is necessary to prevent numerical artifacts in the basis functions. The loss function is a combination of envelope loss and phase loss. Envelopes are computed using the Hilbert transform. Envelope loss is defined as the L1 distance between predicted and true envelopes, while phase loss is calculated as the L1 loss between the real and imaginary components of the waveforms, obtained during the Hilbert transform of the real-valued measurements.

Incident wave removal is applied to the predicted wavefield data to isolate backscattered energy by removing the forward-propagating wave components in the wavenumber-frequency domain using 2D FFT. In this work, we adopt the polar axis method due to its simplicity and ease of implementation. While accurate localization typically requires careful truncation in both time and space domains, our goal is a rapid assessment of the predicted wavefield. Therefore, we perform a full removal of forward-propagating energy in the wavenumber–frequency domain without fine-tuned truncation. The root-mean-square (RMS) energy of the remaining backward-propagating wavefield is then used to identify the presence and location of defects.

NUMERICAL SIMULATION

The dataset used in this study is generated from a numerical simulation of A0 mode Lamb wave propagation in a cylindrical pipe using ABAQUS shown in figure 2. The pipe model is 3 mm thick, 40 cm in length, and has an outer diameter of 15.24 cm. To minimize boundary reflections, 10 cm absorbing layers are applied at both ends of the pipe. The excitation source is positioned 12.5 cm from the left end, and a crack is introduced at 31.25 cm by removing elements to approximate a 15 mm defect. A 415 kHz excitation signal is used, and additional simulation details are provided in [4].

Sensor points are arranged in an 18 × 36 grid, with 2.5 cm spacing along the longitudinal axis and approximately 1.3 cm spacing along the circumferential direction, corresponding to 1/36 πD. The total signal duration is 1.2 milliseconds, sampled at 10 MHz.

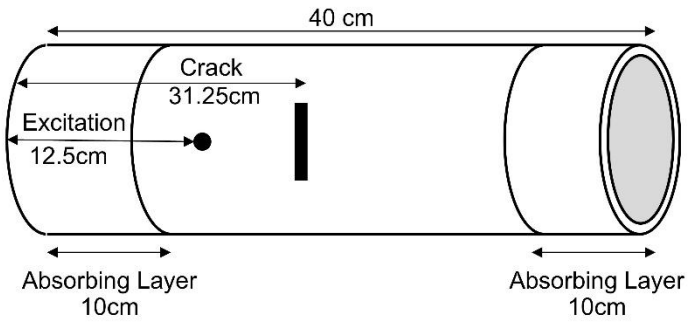

Figure 1. Numerical simulation setup

RESULTS

Figure 3 compares a predicted waveform with the ground truth. The incident wave and the scattered wave caused by the crack are both clearly captured, and the arrival times of the predicted signals align well with the true data. However, a slight phase mismatch is observed. This discrepancy may result from using L1 loss on the waveforms, which provides limited gradient information for optimizing phase alignment, especially given the periodic nature of phase. Despite this, minor phase errors do not significantly impact defect localization, which relies on the RMS energy of the scattered wave.

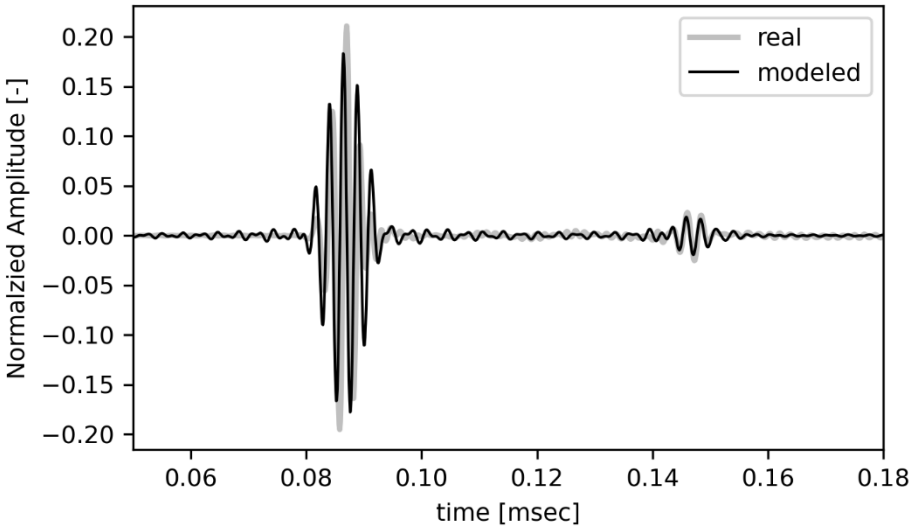

Figure 3. Modeled and real waveform comparison

Figure 4 presents the predicted full wavefield, with white dots indicating the sparse sensor locations used for reconstruction. The model successfully captures the localized scattering behavior, demonstrating its ability to generalize from sparse inputs. A video

of the predicted wavefield evolution, which captures scattering from higher order helical arrivals that are later than the incident wave, is available from the authors upon request.

Finally, Figure 5 shows the RMS energy map after the incident wave has been removed. The high-RMS region corresponds closely with the actual defect location. The observed lobe-shaped pattern in the RMS map is consistent with explanations provided in [4].

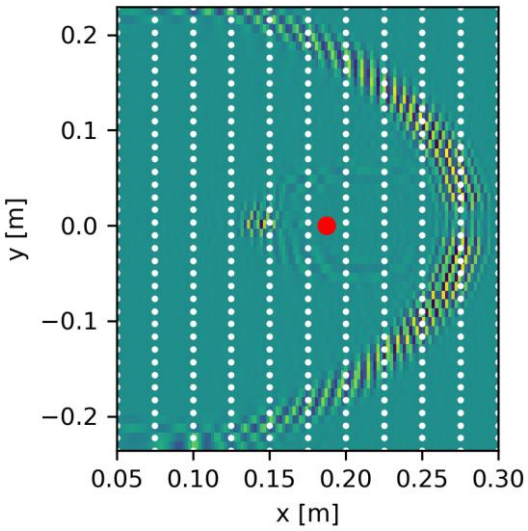

Figure 4. Predicted wavefield with white dots indicating the sensing points and red dot indicating the crack location

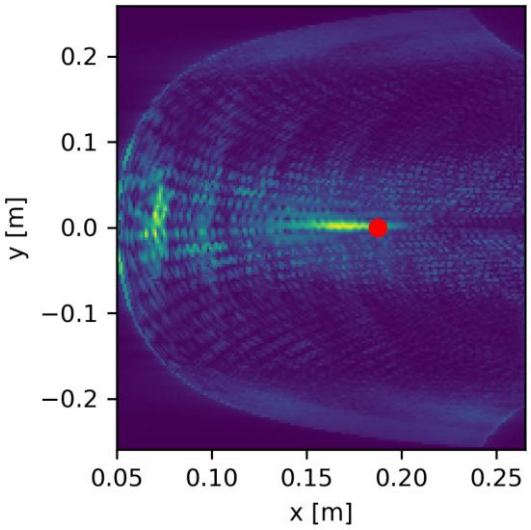

Figure 5. RMS plot on the scattering energy with red dot indicating the crack location

CONCLUSION

This work introduces a baseline-free approach for predicting wavefields and localizing defects in cylindrical structures using sparse sensor measurements. The model leverages a physics-inspired basis function, parameterized to capture key waveform characteristics such as amplitude and phase. By fitting this basis to sparse spatial inputs, the method successfully reconstructs complex wave phenomena, including incident waves, scattered fields, and helical arrivals. Defect localization using the predicted wavefield is achieved by isolating backscattered and computing RMS maps, which closely align with the true defect location. This demonstrates the method's potential for interpretable and efficient structural health monitoring, particularly in settings where sensing is limited.

Future work will explore alternative loss functions that better capture phase behavior to further improve waveform fidelity. In addition, experimental data collection is underway to evaluate the performance and generalizability of the proposed method under real-world conditions.

REFERENCES

1. Livadiotis, S., Lee, G., Wilson, N., & Salamone, S., "Structural Integrity Assessment of Nuclear Spent Fuel Canisters Using Guided Waves," IWSHM 2023
2. Harley, J. B., & Moura, J. M. F. (2013). Sparse recovery of the multimodal and dispersive characteristics of Lamb waves. The Journal of the Acoustical Society of America, 133(5), 2732–2745.
3. Michaels, T. E., Michaels, J. E., & Ruzzene, M. (2011). Frequency–wavenumber domain analysis of guided wavefields. Ultrasonics, 51(4), 452–466.
4. Shivashankar, P., Sohn, J., Salamone, S., "Tracking growth of crack-like defects in hollow cylindrical structures from the stepped-wavelength scattering of helical guided ultrasonic waves," Mechanical Systems and Signal Processing, Volume 236, 2025,112918